

Surface-step-induced magnetic anisotropy of $p(1 \times 1)$ Fe on W(100)

Hector C. Mireles^{a)} and J. L. Erskine^{b)}

Department of Physics, University of Texas at Austin, Austin, Texas 78712-1081

Magneto-optic Kerr effect measurements of ultrathin $p(1 \times 1)$ Fe films on graded-step-density W(100) are used to study step-induced magnetic anisotropy. Spot-profile-analysis low-energy-electron diffraction is used to characterize the stepped W(100) surface prior to film growth and the epitaxial Fe layer after vapor deposition. The experimental results are qualitatively compatible with prior experiments and with theoretical predictions based on the Néel model and on a one-dimensional micromagnetic model proposed by Hyman, Zangwell, and Stiles (HZS). The observed evolution of hysteresis loop shape as a function of step density and anisotropy strength (which was varied by chemisorption of oxygen) is observed to be consistent with a hysteresis loop phase diagram based on the HZS model. However, the measured variation of switching field versus vicinal angle α for 2 monolayer thick Fe films differs significantly from the quadratic dependence predicted by the Néel model and from the dependence predicted by HZS. The surface-step-induced anisotropy vanishes at high vicinality ($\alpha \sim 10^\circ$) and novel two-state switching is observed at specific vicinal angles. © 2001 American Institute of Physics. [DOI: 10.1063/1.1355319]

Reduced symmetry associated with ultrathin films grown on vicinal surfaces is expected to produce uniaxial magnetic anisotropy.¹ This surface-step-induced anisotropy was observed directly, in 1992, in experiments involving ultrathin ferromagnetic films grown on vicinal surfaces of Cu(111)² and W(100).³ The novel magnetic properties and possible technological relevance of surface-step-driven magnetic anisotropy stimulated subsequent experimental work^{4,5} to more thoroughly characterize the phenomena, as well as a few theoretical efforts^{6,7} to understand the experimental results through suitable models.

Chung *et al.*⁶ reported a Néel surface anisotropy model that correctly accounts for general features of surface-step-induced thin film magnetic anisotropy including the difference in anisotropy-driven spin orientation of the Fe/W(100) and Co/Cu(111) systems: spin orientation perpendicular to the step edges for Fe/W(100) and parallel for Co/Cu(111). Subsequent experiments^{4,5} on several vicinal surface systems including Fe on stepped Ag(100), W(100), and Pd(100) have addressed additional specific predictions of the Néel model applied to vicinal surface magnetic anisotropy including quadratic dependence of the anisotropy switching field, H_s , on vicinal angle α , for (bcc) Fe on Ag(100)⁴ and W(100),⁵ and linear dependence for (fcc) Fe on Pd(100).⁴

More recently, Hyman, Zangwill, and Stiles (HZS)⁷ reported a theoretical study of magnetic reversal of ultrathin films on vicinal surfaces based on a one-dimensional micromagnetic model. The HZS model incorporates domain wall

energy involving exchange J , fourfold anisotropy energy (described by K_4) characterizing contributions from fourfold surface sites, and twofold anisotropy energy (described by K_2) characterizing contributions from step-edge atomic sites. Numerical simulations of spin configurations resulting from the model yield predictions of hysteresis loop shapes and plots of switching fields as a function of terrace width L and anisotropy strengths K_4 and K_2 . These predictions allow HZS to introduce and discuss an “anisotropy phase diagram” that catalogs the various allowed magnetic reversal mechanisms and characteristic loop shapes as a function of the relevant parameters: $\Lambda = L/W$ the normalized step width and \mathbf{K} the normalized step anisotropy energy. The terrace width L is normalized to the exchange length $W = \sqrt{J/2K_4}$ and the surface step anisotropy energy $\mathbf{K} = K_2/2\sigma$ is normalized to the domain wall energy $\sigma = \sqrt{2JK_4}$.

The objective of the work described here was to test essential elements of the HZS model and to explore surface-step-induced magnetic anisotropy of the Fe/W(100) system over a wider range of parameters than covered in prior work.^{3,5} The instrumentation and methodology including Kerr effect polarimeter, film growth, and characterization methods have been described in prior publications.^{3,8} The present work employed a graded-step-density W(100) sample that was characterized by spot-profile-analysis low-energy diffraction (SPALEED). The vicinal angle was varied from $\alpha = 0^\circ$ to $\alpha > 18^\circ$. Most of the films studied were 2 monolayer (ML) $p(1 \times 1)$ Fe films that exhibited good epitaxial structure. Oxygen chemisorption was used to vary \mathbf{K} .

Extensive SPALEED studies of our graded-step-density W(100) established the absence of step bunching or roughening resulting from the standard cleaning procedures (annealing in oxygen to eliminate surface carbon followed by

^{a)}Present address: Department of Physics, Trinity University, San Antonio, Texas; electronic mail: hector.mireles@trinity.edu

^{b)}Author to whom correspondence should be addressed; electronic mail: erskine@physics.utexas.edu

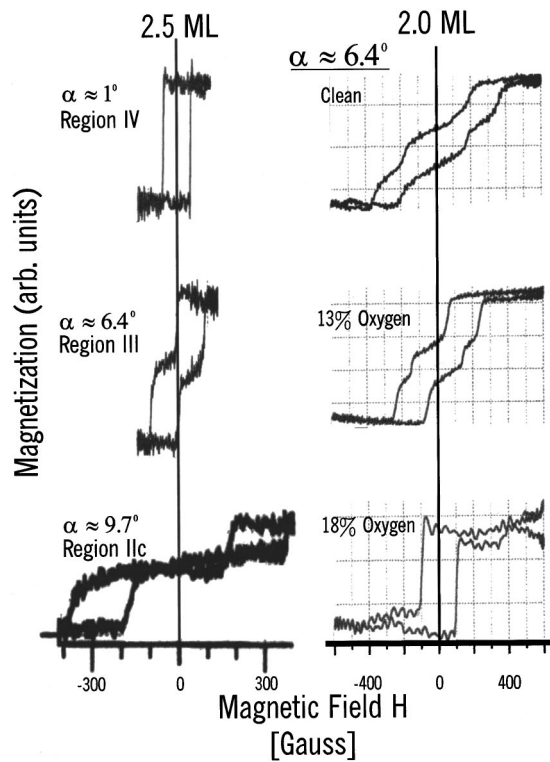


FIG. 1. Selected measured hysteresis loops for $p(1 \times 1)$ Fe on vicinal W(100). (Left) Clean films with vicinal angle α and corresponding region of HZS phase diagram (see Ref. 7) indicated. (Right) Double switching hysteresis loop (see Ref. 9) observed at $\alpha = 6.4^\circ$ and changes resulting from reduced \mathbf{K} when oxygen is adsorbed on the surface.

high-temperature flashing) used to prepare the surface prior to film growth. The SPALÉED profiles also indicated a very sharp distribution of the average number of terrace atoms at the number predicted based on vicinal angle. Auger electron spectroscopy (AES) was used to confirm film thickness (attenuation of W AES lines) and to check surface composition including oxygen coverage after dosing to reduce K_2 . Evidence of preferential oxygen adsorption at steps was observed based on the sensitivity of \mathbf{K} to low oxygen doses.

Figure 1 displays a representative set of measured hysteresis loops for 2 ML $p(1 \times 1)$ Fe on W(100) as a function of vicinal angle α and as a function of oxygen coverage for a fixed vicinal angle. These data illustrate the variation of loop shapes and switching fields that occur as the parameters Λ (terrace width) and \mathbf{K} (step anisotropy energy) are varied. The three loops that illustrate the effect of oxygen (\mathbf{K} variation) were measured at a specific vicinal angle $\alpha = 6.4^\circ$ where novel two-state switching of the film (resulting from step-induced anisotropy) was observed.⁹

Figure 2 displays selected reduced data from our present study and compares the results with two theoretical models. The plotted solid curve shows calculated switching fields H_s versus vicinality obtained from the Néel model⁴ (α^2 dependence). The dashed curve displays results from HZS simulations⁷ for a specific $\mathbf{K} = 0.5$. The shaded region at large vicinal angles shows where the step-induced anisotropy vanishes and loops revert to shapes shown in Fig. 1 for $\alpha \sim 1^\circ$. The inset hysteresis loops show calculated loop

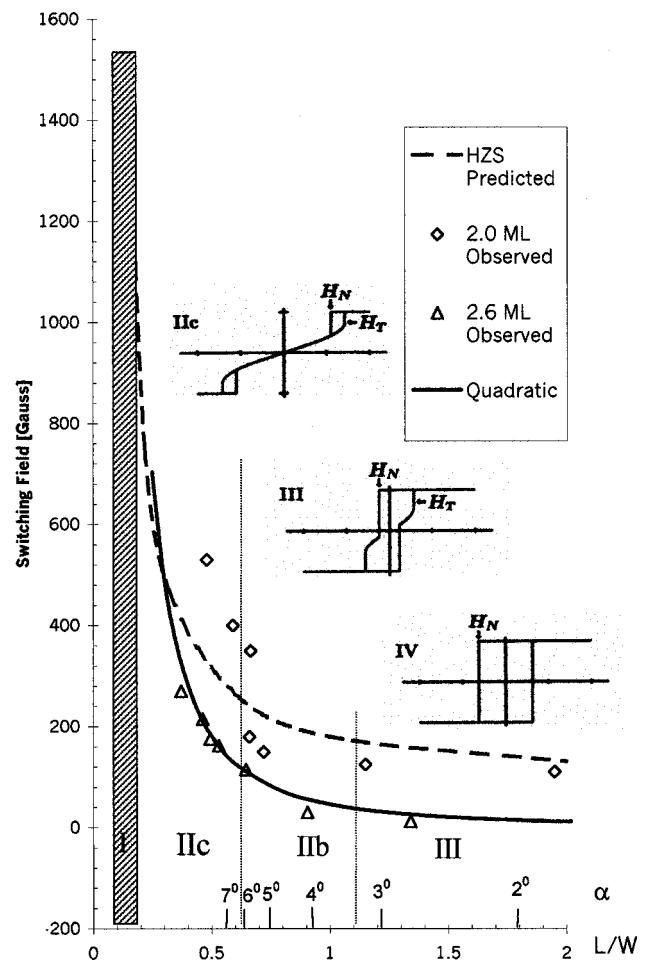


FIG. 2. Graphs of switching field vs vicinal angle α and normalized terrace width Λ . Dashed line, HZS result (see Ref. 7) for $\mathbf{K} = 0.5$; solid line, Néel α^2 dependence. (Insets) HZS calculated loops for three regions of phase diagram. Diamond shaped data points, 2.5 ML $p(1 \times 1)$ Fe film that exhibited double switching at $\alpha = 6.4^\circ$ (refer to Fig. 1). Two switching fields are plotted at $\alpha = 6.4^\circ$. Triangle shaped data points, second set of data for ~ 2.6 ML thick $p(1 \times 1)$ Fe film that did not exhibit strong double switching behavior. Shaded region at small Λ ($\alpha > 18^\circ$) indicates high vicinalities, where step-induced anisotropy vanishes.

shapes⁷ corresponding to specific regions of the HZS hysteresis loop phase diagram. Comparison of calculated and measured loop shapes and switching fields as a function of vicinality (Figs. 1 and 2) suggests that the HZS model captures the basic features of surface-step-induced magnetic anisotropy.

Our experimental results do differ quantitatively in some respects with prior experimental work and with the HZS model. At low vicinalities (i.e., $\alpha < 7^\circ$) prior work yielded $H_s \sim \alpha^2$, in good agreement with quadratic dependence predicted by the Néel model. We obtain a slightly stronger power law dependence $\sim \alpha^{2.6}$ ($\alpha < 7^\circ$) for a series of measurements on films in the 2–3 ML thickness range. We also find a different power law fit for $7^\circ < \alpha < 10^\circ$, and a collapse of H_s above $\alpha = 10^\circ$ as shown in Fig. 2. [This is a very high index beyond (0,1,6).]

We conclude that the Néel model yields accurate predictions of switching field versus α at low vicinalities and that

the HZS model captures many of the qualitative features of surface-step-induced anisotropy. The double switching phenomena observed at $\alpha \sim 6.4^\circ$ can be understood from the dependence of H_s on vicinality. This specific angle is half way between $\alpha = 5.71^\circ$ and $\alpha = 7.12^\circ$, which correspond to $N=5$ and $N=4$ atom terrace widths [surface indices (0, 1, 10) and (0, 1, 8)]. The stepped W(100) surface at this vicinality consists of a sequence of $N=5$ and $N=4$ terraces that yield inequivalent magnetic islands with different switching fields. All films did not exhibit clear double switching features displayed in Fig. 1. Film thickness and crystal order appear to affect the double switching behavior. Oxygen contamination affects H_c of both switching thresholds (Fig. 1). Additional theoretical work is required to refine the models to obtain quantitative predictive capabilities and to account for new step-induced behavior including double switching at specific vicinalities ($\alpha \sim 6.4^\circ$) and vanishing of the anisotropy strength at $\alpha > 10^\circ$.¹⁰

This work was supported by NSF Grant No. DMR 9972113.

¹L. Néel, J. Phys. Radium **15**, 225 (1954).

²A. Berger, U. Linke, and H. P. Oepen, Phys. Rev. Lett. **68**, 839 (1992).

³J. Chen and J. L. Erskine, Phys. Rev. Lett. **68**, 1212 (1992).

⁴R. K. Kawakami, E. J. Escorcia-Aparicio, and Z. Q. Qiu, Phys. Rev. Lett. **77**, 2570 (1996).

⁵H. J. Choi, R. K. Kawakami, E. J. Escorcia-Aparicio, Z. Q. Qiu, J. Pearson, J. S. Jiang, D. Li, R. M. Osgood III, and S. D. Bader, J. Appl. Phys. **85**, 4958 (1999).

⁶D. S. Chuang, C. A. Ballentine, and R. C. O'Handley, Phys. Rev. B **49**, 15084 (1994).

⁷R. A. Hyman, A. Zangwill, and M. D. Stiles, Phys. Rev. B **58**, 9276 (1998).

⁸C. A. Ballentine, R. L. Fink, J. Araya-Pochet, and J. L. Erskine, Appl. Phys. A: Solids Surf. **49**, 459 (1989).

⁹H. C. Mireles and J. L. Erskine, Phys. Rev. Lett. (submitted).

¹⁰M. Getzlaff, R. Pascal, H. Todter, M. Bode, and R. Wiesendanger, Surf. Rev. Lett. **6**, 241 (1999); H. Bethage, D. Hener, Ch. Jensen, K. Reshöft, and V. Köhler, Surf. Sci. **331**, 878 (1995).